PIM kinases phosphorylate lactate dehydrogenase A at serine 161 and suppress its nuclear ubiquitination

Kwan Long Mung[1] (iD), Annika Meinander[2] (iD) and Päivi J. Koskinen[1] (iD)

1 Department of Biology, University of Turku, Finland
2 Faculty of Science and Engineering, Cell Biology, BioCity, Åbo Akademi University, Turku, Finland

Lactate dehydrogenase A (LDHA) is a glycolytic enzyme catalysing the reversible conversion of pyruvate to lactate. It has been implicated as a substrate for PIM kinases, yet the relevant target sites and functional consequences of phosphorylation have remained unknown. Here, we show that all three PIM family members can phosphorylate LDHA at serine 161. When we investigated the physiological consequences of this phosphorylation in PC3 prostate cancer and MCF7 breast cancer cells, we noticed that it suppressed ubiquitin-mediated degradation of nuclear LDHA and promoted interactions between LDHA and 14-3-3 proteins. By contrast, in CRISPR/Cas9-edited knock-out cells lacking all three PIM family members, ubiquitination of nuclear LDHA was dramatically increased followed by its decreased expression. Our data suggest that PIM kinases support nuclear LDHA expression and activities by promoting phosphorylation-dependent interactions of LDHA with 14-3-3ε, which shields nuclear LDHA from ubiquitin-mediated degradation.

Introduction

PIM kinases are a family of serine–threonine kinases with three highly homologous family members (PIM1, PIM2 and PIM3) that are often over-expressed in haematological or solid tumours [1–3] and that contribute to tumorigenesis there [4–6]. The PIM kinases are constitutively active [7] and regulate cell survival, motility, proliferation and metabolism by phosphorylating a wide range of substrates including BAD [8], NFATC1 [9], NOTCH1 [10], NOTCH3 [11], CAPZ [12] and LKB1 [13]. Knocking out all three members of the PIM family results in LKB1-dependent AMPK activation [13,14], increased production of reactive oxygen species as well as altered expression of several metabolic enzymes involved in glycolysis, pentose phosphate pathway or oxidative phosphorylation [15,16]. There is also increasing evidence on the ability of PIM kinases to directly phosphorylate metabolic enzymes, such as lactate dehydrogenase (LDH) [17], enolase [12,17], pyruvate kinase M2 [18], hexokinase 2 [19] and hypoxia-inducible factor 1 [20]. Furthermore, we have previously identified LDH as a putative PIM1-interacting protein in a yeast two-hybrid screen [21]. However, the exact PIM target site(s) in LDH and the functional consequences of PIM-dependent phosphorylation have remained unknown.

Lactate dehydrogenase is a tetrameric enzyme that catalyses the inter-conversion of pyruvate to lactate and NADH to NAD$^+$, enabling sustained glycolysis through NAD$^+$ regeneration [22]. It also catalyses the conversion of α-ketobutyrate (α-KB) to α-hydroxybutyrate (α-HB) with the expense of NADH to NAD$^+$ [23]. The homo- or heterotetrameric LDH complex is composed of protein products encoded by two different genes: LDHA and LDHB. LDHA is also

Abbreviations
KO, knock-out; LDH, lactate dehydrogenase; NAD, nicotinamide adenine dinucleotide; PLA, proximity ligation assay; pSer, phosphoserine; SA, serine (S)-to-alanine (A) phosphomutant; TKO, triple knock-out; Ub, ubiquitin; WT, wild-type; αHB, α-hydroxybutyrate; αKB, α-ketobutyrate.

called the M isoform, as it is the dominant isoform found in skeletal muscle, while LDHB is called the H isoform and is predominantly found in the heart [24]. Over-expression of LDHA is observed in various cancers [22,25,26], where it contributes to resistance towards chemotherapies [27,28]. Upregulation of LDHB is found in aggressive basal-like and triple-negative breast cancers [29,30]. However, in several cases, silencing of LDHB expression via promoter methylation is also observed [22].

Cellular activities of LDHA are heavily regulated by post-translational modifications. Acetylation of LDHA at K5 residue promotes LDHA degradation via autophagy through interaction with HSC70 [31]. On the contrary, succinylation of LDHA at K222 decreases its lysosomal degradation [32]. FGFR1 increases LDHA enzymatic activities through phosphorylation of Y10 and Y83, promoting the formation of active LDHA tetramers and increasing the binding of the NADH substrate, respectively [33]. In addition, both HER2 and SRC phosphorylate LDHA at Y10 and thereby contribute to the metastatic potential of tumours [34].

Lactate dehydrogenase A has been suggested to be protected by 14-3-3 proteins from ubiquitin-dependent degradation [35]. The 14-3-3 protein family consists of seven isoforms (β, γ, ϵ, η, σ, τ and ζ) that interact with phosphorylated proteins and subsequently modulate cellular signalling [36–38]. For example, PIM-dependent phosphorylation of BAD prevents its pro-apoptotic effects as it becomes sequestered by 14-3-3 [8,39]. In this study, we analysed phosphorylation of LDHA in more detail and identified Ser161 as the major target site for PIM kinases. We also observed that PIM-induced phosphorylation of LDHA is essential for its interaction with 14-3-3 and for its protection from ubiquitination. By contrast, knocking out all three PIM kinase members by CRISPR/Cas9-based editing increased ubiquitination and decreased nuclear LDHA expression in both PC3 prostate and MCF7 breast cancer cells. All these data suggest that nuclear LDHA expression is modulated by activities of both the PIM and 14-3-3ϵ proteins.

Results

Nuclear LDHA expression and activities are decreased in the absence of PIM kinases

As we and others had previously reported that PIM kinases bind to LDHA and phosphorylate it *in vitro* [17,21], we wanted to investigate the putative physiological effects of PIM kinases on LDHA expression or activity in a cellular context. For this purpose, we used both PC3 prostate and MCF7 breast cancer cells as well as their derivatives, from which we had knocked out the expression of all three PIM family members by CRISPR/Cas9 genomic editing [13]. For both cell lines, we had established two independent triple knock-out clones (TKO#1 and TKO#2) that provide useful models to study PIM-dependent cellular functions.

When we analysed LDHA protein and mRNA expression levels by western blotting and quantitative PCR, respectively, we did not observe any statistically significant differences between whole-cell lysates of wild-type (WT) and TKO clones of either PC3 or MCF7 cells (Fig. 1A). However, when we performed subcellular fractionations to separate whole-cell lysates into cytosolic and nuclear fractions, significant differences in expression of nuclear LDHA were observed in both PC3 and MCF7 cells (Fig. 1B). There LDHA protein expression was consistently decreased in the nuclear, but not cytosolic fractions of TKO clones as compared to WT cells.

We then analysed the activity of LDHA by measuring its abilities to convert pyruvate to lactate as well as α-ketobutyrate (αKB) to α-hydroxybutyrate (αHB) with the exchange of NADH to NAD^+ (Fig. 2A). In line with the protein expression levels, we did not observe any statistically significant changes in either lactate or αHB production between whole-cell lysates of WT and TKO clones (Fig. 2A). By contrast, when we compared LDHA activities between cytosolic and nuclear fractions, we detected dramatically decreased LDHA activities in terms of production of lactate and αHB in nuclear, but not cytoplasmic fractions of TKO clones as compared to WT cells (Fig. 2B). The cytosolic LDHA activities were on average 25- to 50-fold higher than those of nuclear fractions, which correlated well with the observations that prolonged exposures were required to detect LDHA protein in nuclear fractions (Fig. 1C). Therefore, due to the overwhelming amount of LDHA present in cytosolic fractions compared to nuclear fractions, it was evident that examination of whole-cell lysates did not enable detection of any nuclear-level changes in LDHA activity. Ultimately, the aforementioned results indicate that both expression and activity of nuclear LDHA are reduced in PIM-deficient cells.

PIM kinases phosphorylate LDHA at serine 161 residue

Having observed PIM-dependent physiological effects on LDHA activities, we proceeded to examine cellular interactions between PIM kinases and LDHA in more
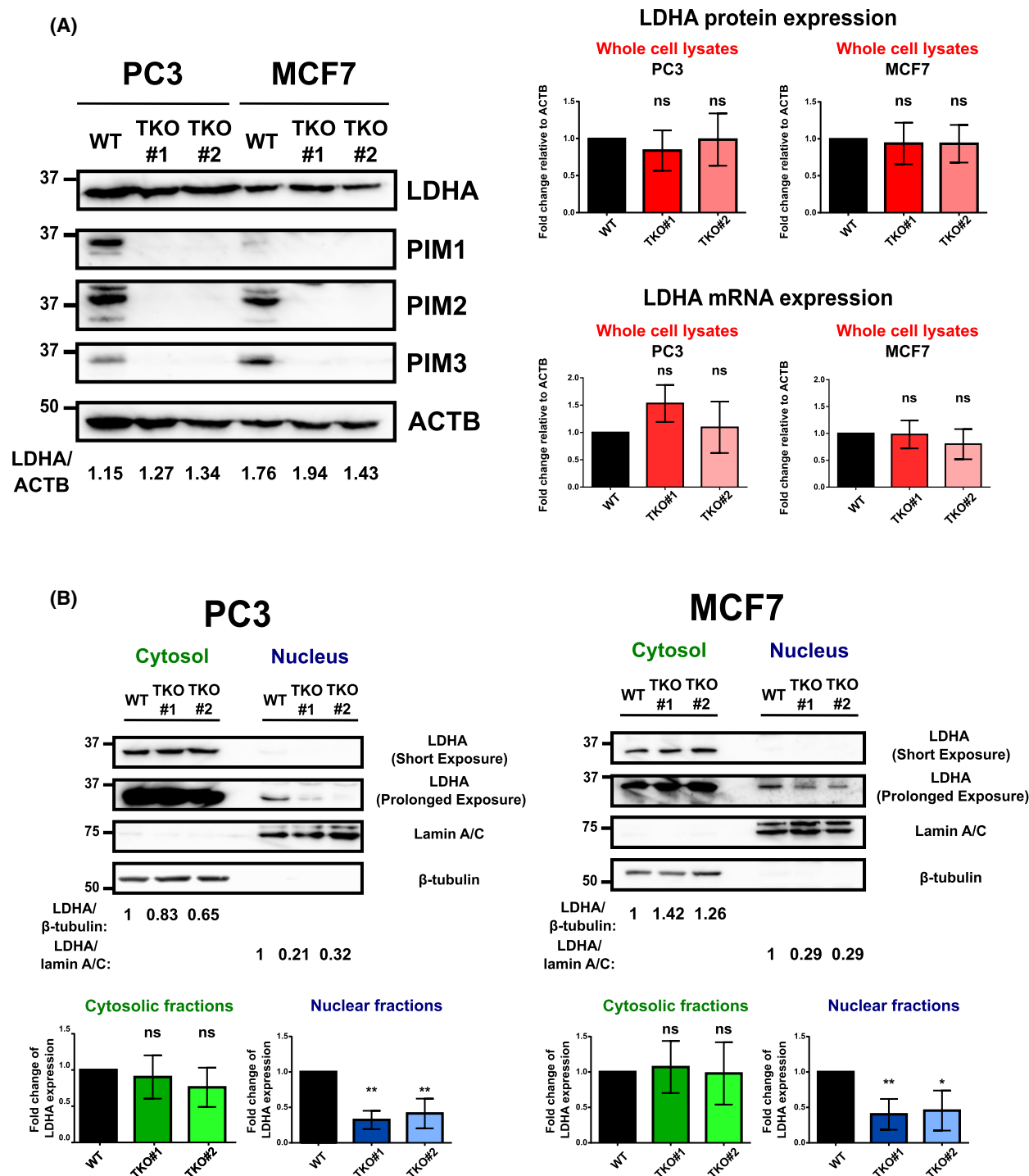
Fig. 1. Inactivation of PIM kinases decreases nuclear LDHA expression. (A) LDHA and PIM protein expression levels were examined by western blotting from wild-type (WT) PC3 and MCF7 cells and their triple knock-out (TKO#1 and TKO#2) derivatives lacking all three PIM kinases, while LDHA mRNA expression levels were measured by quantitative PCR. (B) Cytosolic and nuclear LDHA protein expression levels were similarly analysed. β-tubulin and lamin A/C were used as markers for the cytosolic and nuclear fractions, respectively. Shown are representative images as well as bar charts with relative expression levels of LDHA in TKO cells as compared to WT cells (average values ± SD, n = 3). Student's t-test was used to determine the statistical significance. Significant differences (P < 0.05 and P < 0.01) were marked with * and **, respectively; ns refers to no significance. Error bars represent standard deviations.
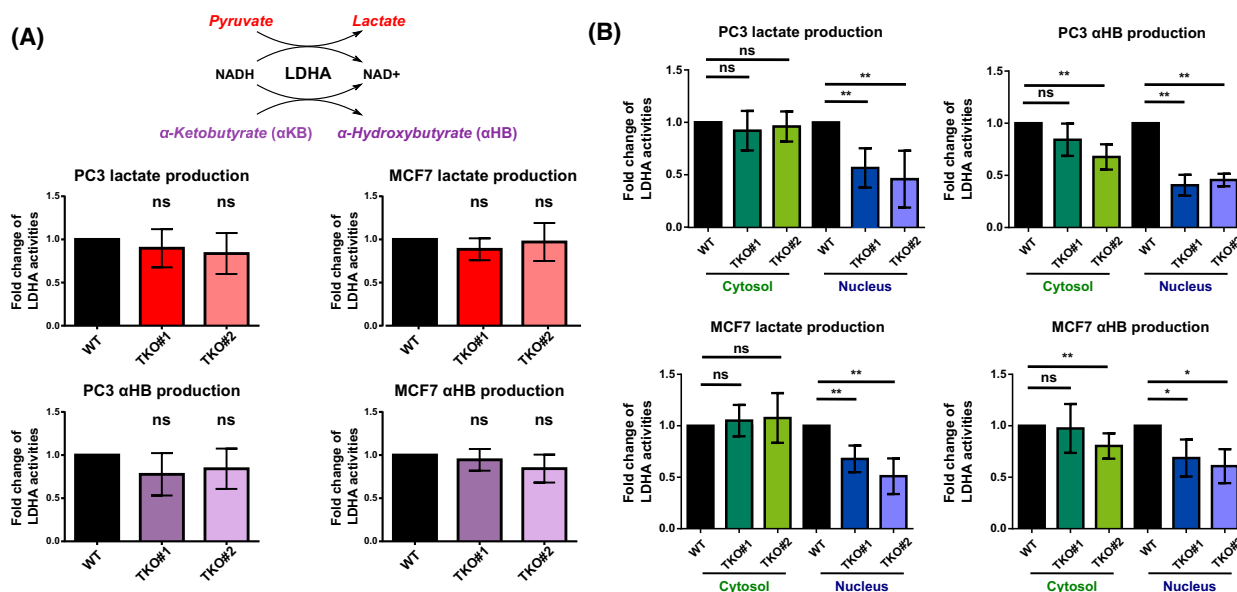
Fig. 2. Inactivation of PIM kinases decreases nuclear LDHA activities. (A) Cellular LDHA activities corresponding to the rate of conversion from pyruvate to lactate or from α-ketobutyrate (αKB) to α-hydroxybutyrate (αHB) were measured from cell lysates of PC3 or MCF7 WT and TKO cells. Results were normalized with total protein and plotted as bar charts with relative activities of TKO cells as compared to WT cells (average values ± SD, $n = 3$). (B) Bar charts with relative cytosolic and nuclear LDHA activities in TKO cells as compared to WT cells (average values ± SD, $n = 3$). Student's t-test was used to determine the statistical significance. Significant differences ($P < 0.05$ and $P < 0.01$) were marked with * and **, respectively; ns refers to no significance. Error bars represent standard deviations.

detail. Using both proximity ligation assays (Fig. 3A) and co-immunoprecipitation experiments (Fig. 3B,C) with PC3 cell samples, we demonstrated that endogenously expressed PIM1 and LDHA physically interact with each other in WT, but not TKO cells. Moreover, we observed that serine phosphorylation levels of immunoprecipitated LDHA were significantly lower in TKO clones of both PC3 and MCF7 cells as compared to WT cells (Fig. 3D), suggesting that the serine/threonine-specific PIM kinases phosphorylate LDHA within cells. To confirm this conclusion, we performed radioactive *in vitro* kinase assays with PIM and LDHA proteins. For this purpose, both types of proteins were produced in bacteria as fusions with glutathione S-transferase (GST), but the GST-tag was later removed from LDHA. The results of the kinase assays indicated that all three PIM kinases are capable of phosphorylating LDHA *in vitro*, while LDHA does not autophosphorylate itself (Fig. 3E).

To reveal the PIM target sites, we performed in-gel digestion of *in vitro* phosphorylated LDHA followed by mass spectrometry analysis. Based on this analysis, serine residues 79, 105 and 161 were identified as potential PIM target sites on LDHA. In addition, *in silico* analysis of LDHA indicated that the amino acid sequence around serine 319 (LKKSA) aligns relatively

well with the PIM1-targeted consensus sequence (K/R-K/R-R-K/R-L-S/T-a; a = a small = 0 chain amino acid) [40]. Therefore, we used site-directed mutagenesis to change the four putative PIM-targeted serine residues to alanines. Radioactive kinase assays with phospho-deficient mutants revealed that S161 and S319 are the major *in vitro* target sites for PIM1 on LDHA (Fig. 3F).

Next, we pursued verifying the PIM target sites on LDHA within cells. For this purpose, PC3 WT and TKO#1 cells were transfected with plasmids expressing either WT LDHA tagged with the green fluorescent protein (GFP), or one of the corresponding phospho-deficient mutants, S161A or S319A. When cell lysates were immunoprecipitated with GFP antibodies and immunoblotted with phospho-serine antibodies, there was a significant decrease in the level of LDHA phosphorylation in TKO cells as compared to WT cells (Fig. 3G). By contrast, the S161A mutation reduced the phosphorylation level of LDHA also in WT cells close to that observed in TKO cells, while the S319A mutation was less effective. Thus, by combining both *in vitro* and cellular data, it can be concluded that S161 is the major physiologically relevant PIM phosphorylation site on LDHA.

PIM-induced phosphorylation of LDHA suppresses its ubiquitination

While searching for the mechanism to explain the lower nuclear expression levels of LDHA in TKO cells as compared to WT cells, we noticed that LDHA was abnormally highly ubiquitinated in TKO clones. This was consistently observed in PC3-derived cells transiently over-expressing HA-tagged ubiquitin when either endogenous LDHA (Fig. 4A) or co-over-expressed FLAG-tagged LDHA protein (Fig. 4B) was immuno-precipitated and stained with HA, LDHA or FLAG antibodies. The results from subcellular fractionation experiments with TKO cells based on PC3 or MCF7 (Fig. 4C) indicated that the ubiquitinated LDHA was predominantly localized in the nuclear fraction. The nuclear ubiquitination was suppressed by transient over-expression of His-tagged PIM1 (Fig. 4D), confirming the protective role of PIM kinases there. Furthermore, mutation of the PIM-targeted serine 161 of LDHA into alanine was sufficient to induce nuclear LDHA ubiquitination in PC3 WT cells, while the corresponding mutation of serine 319 had no major effects (Fig. 4E). These data suggest that S161 is the key site for PIM-dependent protection of LDHA from nuclear ubiquitination. In addition, subcellular fractionation experiments confirmed that the ubiquitination triggered by the S161A mutation in WT cells was enriched in the nuclear fraction, similar to what was seen with WT LDHA in TKO clones (Fig. 4F).

Next, we immunoprecipitated FLAG-tagged LDHA from PC3 WT and TKO cells and blotted the samples with antibodies against the K48-specific polyubiquitin chains, which are known to be associated with proteasomal degradation [41]. While K48 ubiquitin was also observed in WT cells, its conjugation to LDHA was strongly enhanced in TKO cells (Fig. 4G) as well as in WT cells expressing the S161A mutant of FLAG-tagged LDHA (Fig. 4H), suggesting that phosphorylation of LDHA at serine 161 suppresses its K48-linked polyubiquitination.

To determine, whether a lack of PIM-dependent phosphorylation affected LDHA protein conformation and thereby increased its susceptibility to ubiquitination, we performed protein crosslinking assays with glutaraldehyde. However, we did not observe any significant differences in the amounts of endogenously expressed LDHA monomers, dimers or tetramers between PC3 WT and TKO cells (Fig. 4I), or between ectopically expressed flag-tagged WT LDHA and the S161A mutant (Fig. 4J). Thus, the observed effects on ubiquitination cannot be explained by differences in LDHA protein folding and oligomerization.

14-3-3 proteins are also essential for the suppression of LDHA ubiquitination

As 14-3-3 proteins had recently been reported to suppress LDHA ubiquitination [35], this prompted us to investigate interactions between LDHA and 14-3-3 proteins in WT and TKO clones. Performing proximity ligation assays with PC3 cell samples together with LDHA and pan-14-3-3 antibodies, we demonstrated that endogenously expressed LDHA and 14-3-3 proteins physically interact with each other in WT cells, but not in PIM TKO clones (Fig. 5A). Also, in co-immunoprecipitation experiments with PC3 or MCF7 cell samples, much less LDHA was pulled down together with 14-3-3 proteins in TKO clones as compared to WT cells (Fig. 5B). These data suggest that PIM-dependent phosphorylation of LDHA is required to maintain interactions between LDHA and 14-3-3 proteins. More specifically, we observed that transiently over-expressed FLAG-tagged WT LDHA bound strongly with HA-tagged 14-3-3ε in WT PC3 cells, but not in TKO cells, while the S161A mutation in LDHA decreased the interaction also in WT cells (Fig. 5C). Furthermore, we observed that transient over-expression of 14-3-3ε partially suppressed LDHA ubiquitination in PC3 TKO cells (Fig. 5D), resulting in slightly increased nuclear expression of LDHA (Fig. 5E). These effects may be explained by our observations, according to which there was some residual binding between LDHA and endogenously or ectopically expressed 14-3-3 proteins also in the absence of LDHA phosphorylation (Fig. 5B,C). Yet, the striking differences between phosphorylated and non-phosphorylated samples indicate that PIM-induced phosphorylation of LDHA at S161 is vital for the interaction between LDHA and 14-3-3ε proteins and thereby for the ability of 14-3-3 proteins to protect nuclear LDHA from ubiquitin-mediated degradation.

Discussion

Despite several reports on the presence of LDHA in the nucleus [23,25,28,42–44], it has conventionally been depicted as a cytosolic enzyme. Notably, immunohistochemistry stainings have revealed both cytoplasmic and nuclear LDHA expression in lung cancer cells [25,28]. In addition, transmission electron microscopy experiments have confirmed the existence of LDHA in the nucleus of Hela cells [44]. Here, we have observed that LDHA is expressed in both cytosolic and nuclear fractions of PC3 prostate and MCF7 breast cancer cells. However, the majority of LDHA proteins and their activities are located in cytosolic fractions, which

(A) PC3 PIM1 + LDHA

(B) PC3

(C) PC3

(D) PC3 / MCF7

(E)

(F)

(G) PC3
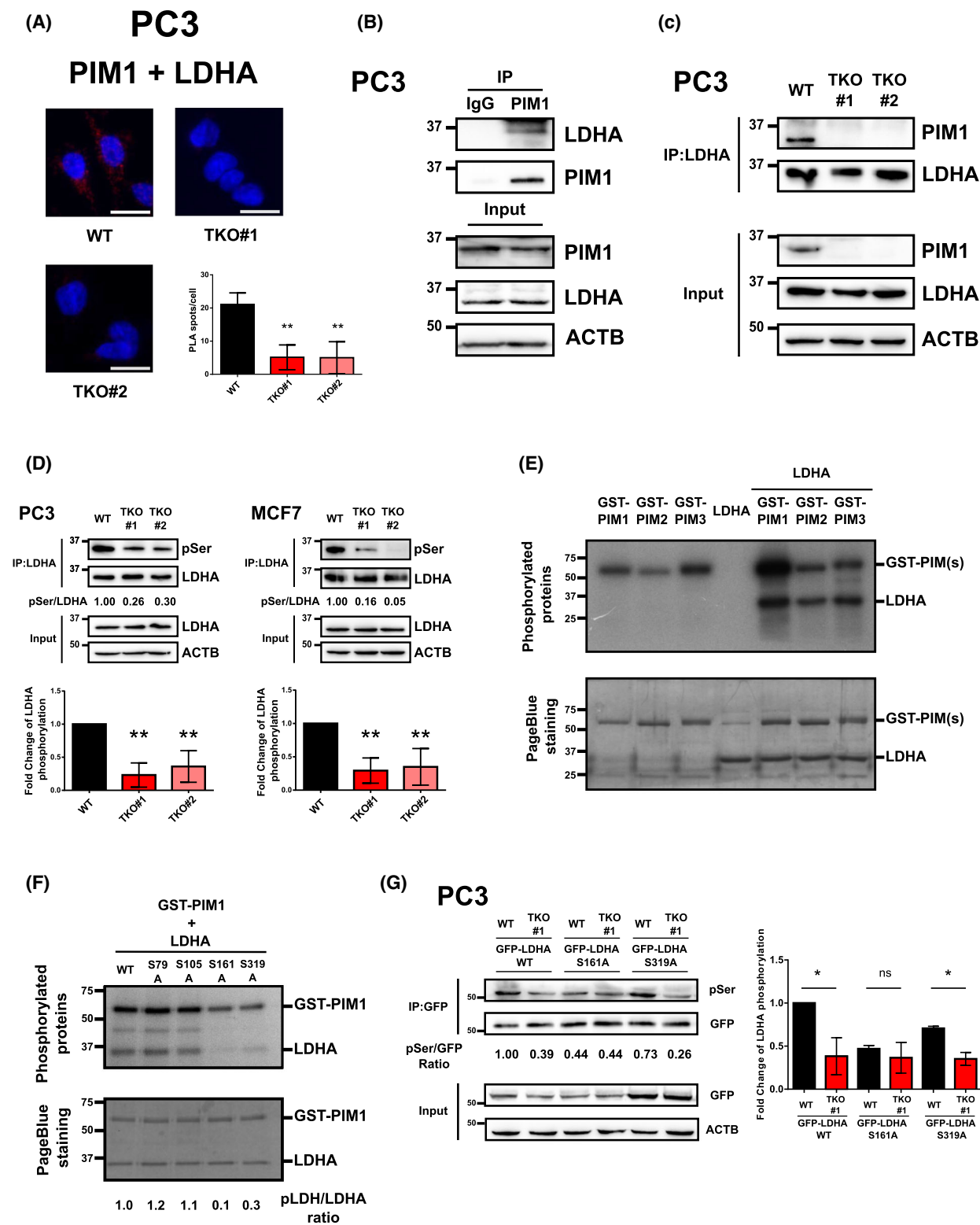
is in agreement with previous observations, e.g. from PC12 cells [43]. So far, there are at least two independent reports on the phosphorylation of LDHA at both

serine and tyrosine residues [42,43]. While the functional consequences of tyrosine phosphorylation of LDHA have been actively explored [33,34], studies on

Fig. 3. PIM kinases interact with LDHA inside cells and phosphorylate it at Ser161. (A) Proximity ligation assays (PLA) were performed to demonstrate physical interactions between endogenously expressed PIM1 and LDHA proteins in WT, but not PIM-deficient (TKO#1 and TKO#2) PC3 cells. Shown are representative images and quantification from PLA assays with anti-PIM1 and anti-LDHA antibodies (Scale bar = 5 μm). For immunoprecipitation analyses, PC3 WT and TKO cell lysates were immunoprecipitated and the blotted samples were stained with indicated antibodies. Ten per cent of each cell lysate had been set aside and stained with indicated antibodies to control for the input amounts of proteins. (B) Co-IP of endogenous LDHA protein with IgG or PIM1 antibodies in WT cells. (C) Co-IP of endogenous PIM1 with LDHA antibodies in WT or TKO cells. (D) Relative serine phosphorylation levels of LDHA in TKO cells as compared to WT cells. Shown are representative images as well as bar charts (average values ± SD, n = 3). (E) Radioactive in vitro kinase assays were performed by incubating GST-PIMs and/or LDHA in the presence of ^{32}P-ATP. Phosphorylated proteins were visualized by autoradiography (upper panel) and protein loading by Page Blue staining (lower panel). Shown is a representative image out of two repeated experiments. (F) Radioactive in vitro kinase assays were performed by incubating GST-PIM1 with different LDHA mutants (S79A, S105A, S161A and S319A). (G) PC3 WT and TKO cells were transiently transfected with plasmids expressing GFP-LDHA (WT, S161A or S319). After 24 h, cell lysates were immunoprecipitated with GFP antibodies and blotted samples were stained with indicated antibodies. Shown are representative images as well as bar charts with relative serine phosphorylation levels of LDHA in TKO cells as compared to WT cells (average values ± SD, n = 3). Student's t-test was used to determine the statistical significance. Significant differences (P < 0.05 and P < 0.01) were marked with * and **, respectively; ns refers to no significance. Error bars represent standard deviations.

serine phosphorylation are lagging behind. In this report, we have focused on PIM-dependent serine phosphorylation of LDHA and identified serine 161 as the major physiologically relevant PIM target site. In high-throughput phosphoproteomic analyses, this site has been found to be phosphorylated under in vivo conditions, but the regulatory kinases and the functional consequences have remained unknown [45]. However, here we revealed two important roles for this phosphorylation, as according to our data it supports interactions between LDHA and 14-3-3ε and thereby protects nuclear LDHA from undergoing K48-mediated ubiquitination and subsequent degradation.

Lactate dehydrogenase A ubiquitination has been observed in AGS gastric cancer cells [32], PLC liver cancer cells exposed to MG132 treatment [35], L6 muscle and COS7 kidney cells exposed to oxidative stress as well as skeletal muscles of rats taken to space-flights [46]. Here, we show that K48-mediated ubiquitination of LDHA occurs predominantly in the nuclear fractions of both PC3 and MCF7 knock-out cells lacking expression and activity of PIM kinases. It has been reported that shRNA knockdown of 14-3-3ζ in HEK293T cells results in robust LDHA ubiquitination, while binding between 14-3-3 proteins and LDHA protects it from ubiquitination [35]. Even more interestingly to us, binding between LDHA and 14-3-3ζ was shown to depend on the phosphorylation status of LDHA, but the critical LDHA phosphorylation site(s) and corresponding upstream kinase(s) remained unknown. Here, we show that the interaction between LDHA and 14-3-3ε proteins is strictly regulated by PIM-dependent phosphorylation of S161 on LDHA. Although over-expressed 14-3-3ε partially suppresses LDHA ubiquitination, it cannot fully restore nuclear LDHA expression in PIM-deficient cells, most likely due to its remarkably reduced capacity to bind to

unphosphorylated LDHA. While our study was ongoing, a multi-subunit complex of E3 ligases was reported to be involved in the ubiquitination of LDHA [47]. Given the existence of examples on 14-3-3 proteins suppressing ubiquitination by shielding binding of E3 ubiquitin ligases to their substrates [48], it would be of interest to determine whether the E3 ligase complex is involved in the nuclear LDHA ubiquitination observed in PIM-deficient cells. Ultimately, all these data suggest that the expression and activities of both PIM kinases and 14-3-3ε proteins are involved in the regulation of nuclear LDHA expression, while further studies are required to examine the possibilities of the involvement of other 14-3-3 isoforms.

In line with the ubiquitination pattern, knocking out all three PIM family members in PC3 and MCF7 cells resulted in decreased nuclear LDHA expression, but no appreciable changes in cytosolic LDHA expression. Even though only a minority of cellular LDHA proteins reside in the nucleus, several important roles for nuclear LDHA have been proposed. For example, it serves as a transcription factor to support histone H2B expression in S-phase [49,50]. In addition, the α-HB metabolite generated by nuclear LDHA promotes the upregulation of H3K79 trimethylation as well as the expression of antioxidant and Wnt target genes [23]. Recently, it has also been found that lactate serves as a substrate for histone lysine lactylation [51], and that elevated histone lactylation levels are associated with poor survival of cancer patients [52]. While increased amounts of exogenous glucose or lactate eventually lead to increased histone lactylation levels [51], mice with enforced nuclear LDHA expression display larger tumour volumes than mice with enforced cytoplasmic LDHA expression, suggesting a tumour-promotive role for nuclear LDHA [23]. Conversely, inhibition of PIM kinases decreases nuclear LDHA expression and also
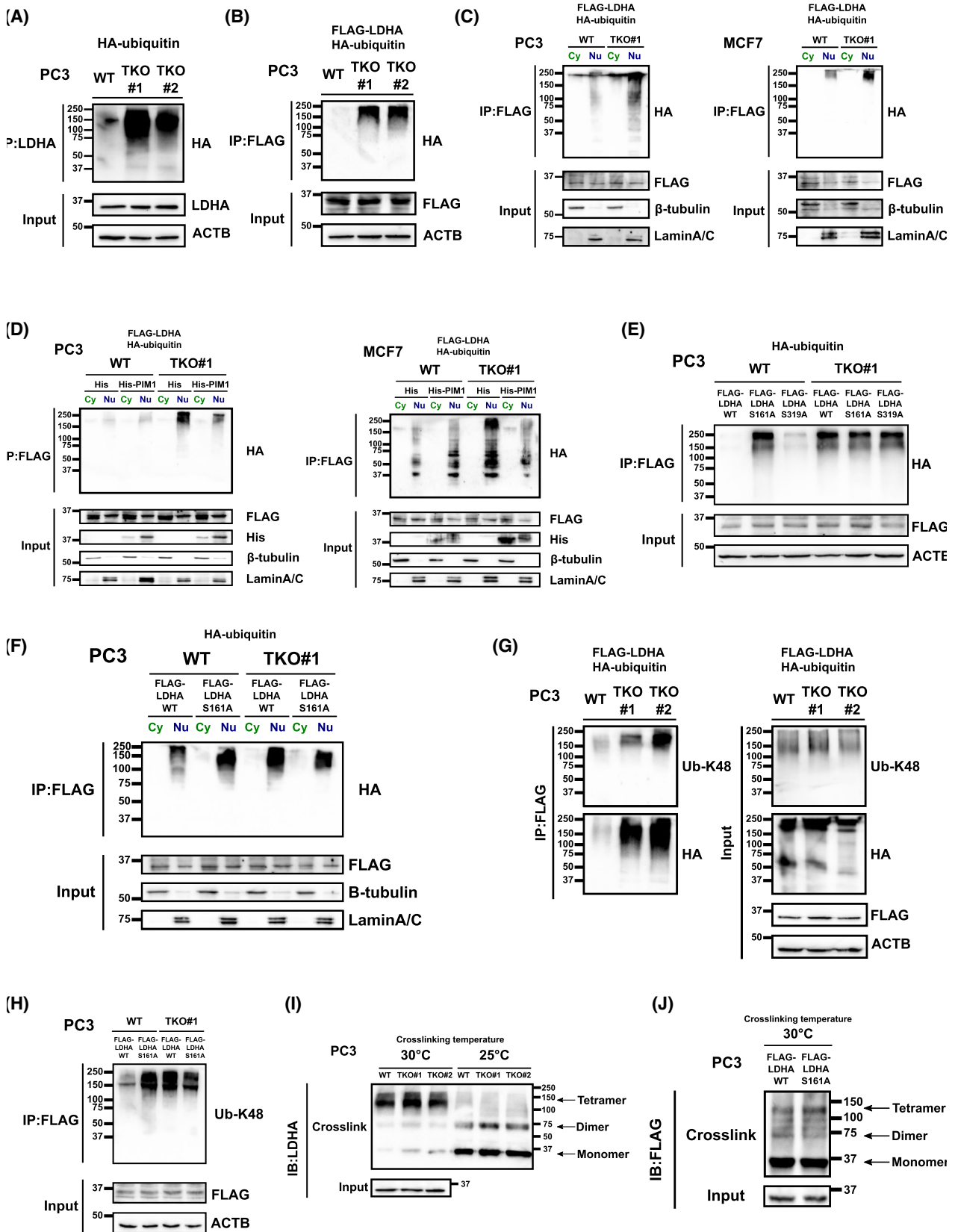
Fig. 4. PIM-induced phosphorylation of LDHA protects it from ubiquitination. PC3 or MCF7 WT and TKO cells were transiently transfected with indicated plasmids expressing HA ubiquitin, WT or mutant FLAG-tagged LDHA, His-tag and/or His-tagged PIM1. After 24 h, cell lysates were immunoprecipitated (IP) and blotted samples were stained with indicated antibodies. Ten per cent of each cell lysate had been set aside and stained with indicated antibodies to control for the input amounts of proteins. Shown are co-IPs of HA ubiquitin with (A) endogenously expressed LDHA, (B) ectopically expressed FLAG-LDHA ($n = 3$), (C) FLAG-LDHA from cytosolic (Cy) and nuclear (Nu) fractions ($n = 3$), (D) FLAG-LDHA from His- or His-PIM1-expressing fractionated cells, (E) FLAG- LDHA (WT, S161A or S319A) ($n = 2$) and (F) FLAG-LDHA (WT, S161A) from fractionated cells ($n = 2$). Presence of K48-specific polyubiquitin chains was similarly analysed from co-IPs with (G) FLAG-LDHA ($n = 3$) (H) or FLAG-LDHA (WT or S161A) ($n = 2$). The oligomerization status of LDHA was analysed by crosslinking assays with glutaraldehyde from (I) WT and TKO cells or (J) from WT cells expressing FLAG-tagged LDHA (WT or S161A).
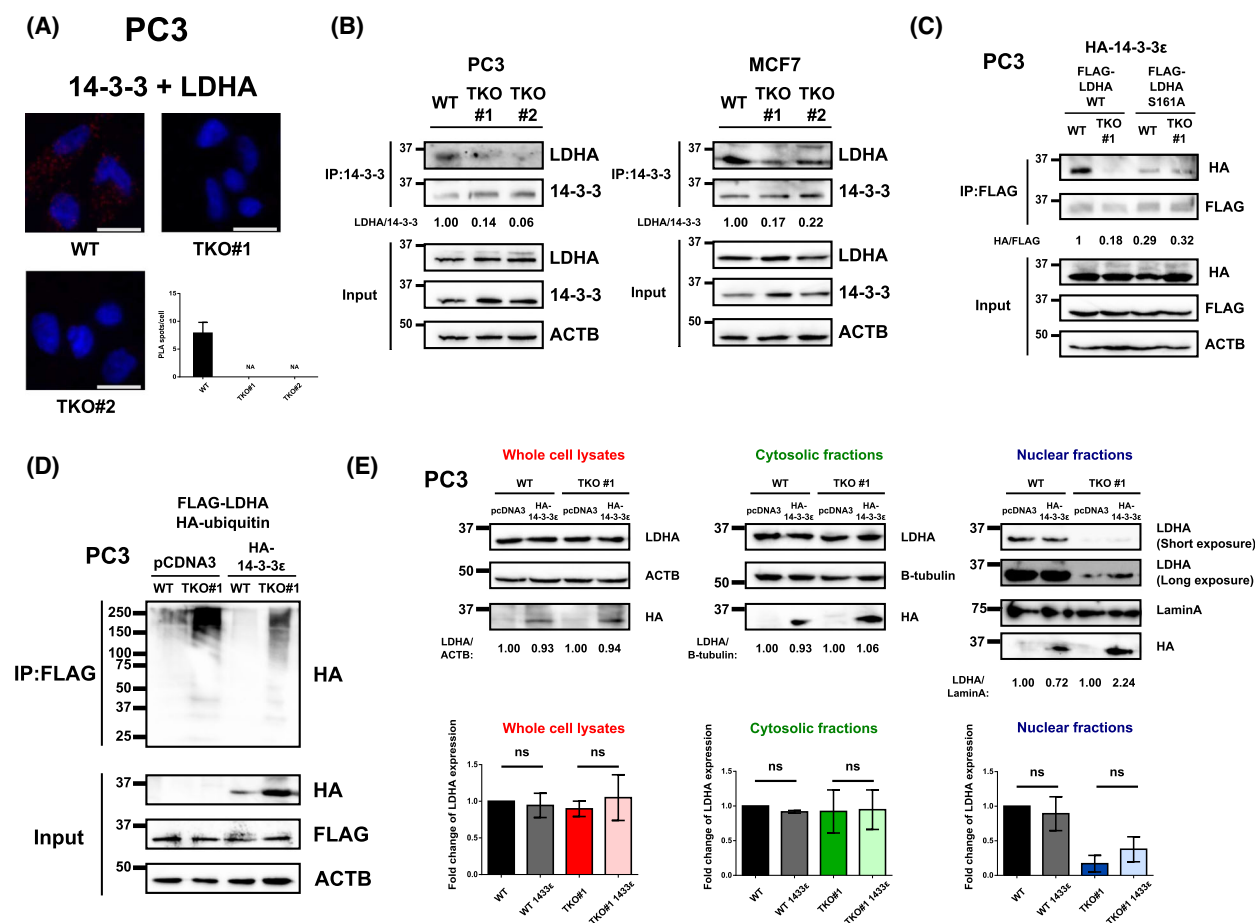
Fig. 5. PIM-induced phosphorylation of LDHA is essential for its interaction with 14-3-3ε. (A) Proximity ligation assays (PLA) were performed to demonstrate the physical interactions between endogenously expressed LDHA and 14-3-3 proteins in WT, but not PIM-deficient (TKO#1 and TKO#2) PC3 cells. Shown are representative images and quantification from PLA assays with anti-LDHA and anti-pan-14-3-3 antibodies (Scale bar = 5 μm). For additional interaction studies, PC3 WT and TKO cells were used as such or transiently transfected with indicated plasmids expressing WT or mutant FLAG-tagged LDHA, HA tag, HA-tagged 14-3-3ε and/or HA ubiquitin. After 24 h, cell lysates were immunoprecipitated (IP) and blotted samples stained with indicated antibodies. Ten per cent of each cell lysate had been set aside and stained with indicated antibodies to control for the input amounts of proteins. (B) Co-IP of endogenous LDHA with endogenous 14-3-3 proteins ($n = 3$). (C) Co-IP of HA-14-3-3 ε with FLAG-LDHA (WT or S161A). (D) Co-IP of HA ubiquitin with FLAG-LDHA ($n = 3$). (E) LDHA expression in whole-cell lysates or cytosolic and nuclear fractions of WT and TKO#1 cells. Shown are representative images of western blots as well as bar charts with relative LDHA expression of each fraction as compared to mock-transfected cells (average values ± SD, $n = 3$). Student's t-test was used to determine the statistical significance. Significant differences ($P < 0.05$ and $P < 0.01$) were marked with * and **, respectively; ns refers to no significance. Error bars represent standard deviations.

decreases tumour size in tumour-bearing mice [2,53]. Thus, in future studies, it would be of interest to dissect the impact of PIM inhibition on LDHA nuclear activities, such as histone methylation and histone lactylation, as such studies may help to establish a rationale for targeting nuclear LDHA as a novel therapeutic option for patients.

Materials and methods

Cell culture reagents and DNA constructs

MCF7 breast cancer and PC3 prostate cancer cells were obtained from American Type Culture Collection (Manassas, VA, USA), and were cultured in Dulbecco's modified Eagle's medium (DMEM) and RPMI-1640 medium (Sigma-Aldrich, St. Louis, MI, USA) respectively. Both media were supplemented with L-glutamine, 10% fetal bovine serum and antibiotics. MEM Non-Essential Amino Acids (Gibco, #11140050; Thermo Fisher Scientific, Waltham, MA, USA) and Sodium Pyruvate (Gibco, #11360070; Thermo Fisher Scientific) were further added to RPMI-1640-based medium for PC3 cells to facilitate cell growth. FuGENE® HD Transfection Reagent (Promega, Madison, WI, USA) was used for plasmid transfections according to the manufacturer's protocol. The use of CRISPR/Cas9-based genome editing to prepare knock-out derivatives of MCF7 and PC3 cells lacking all three members in the PIM family has previously been described [13]. Eukaryotic and bacterial vectors pcDNA™3.1/V5-His-C and pGEX-6P-1 for expression of wild-type (WT) human PIM kinases have been described previously [10]. Expression vectors pcDNA3-HA-14-3-3ε (Addgene Europe, Teddington, UK, #13272) and HA ubiquitin (Addgene Europe, #18712) were kind gifts from Cecilia Sahlgren (Åbo Akademi University, Finland) and Jukka Westermarck (University of Turku, Finland) respectively. Human LDHA was cloned into pGEX-6P-1 (GE Healthcare Life Sciences, Little Chalfont, UK), pFLAG-CMV2 (#E7033, Sigma-Aldrich) and pEGFP-C2 vectors (Clontech Laboratories Inc., Takara Bio USA, San Jose, CA, USA). Site-directed mutagenesis of LDHA was performed using Ultra Pfu DNA Polymerase (Stratagene, San Diego, CA, USA) according to the manufacturer's protocol. The primers used are described in Table S1.

Expression of GST-tagged or His-tagged fusion proteins in *Escherichia coli*

pGEX-6P-1 plasmids (expressing GST-PIMs and GST-LDHAs) were transformed into BL21 *E. coli* strain for protein production. Overnight bacterial cultures were grown at 30 °C until OD_{600} of 0.6. Isopropyl-β-D-galactosidase (250 μM; Sigma-Aldrich) was added to induce protein expression, and the cells were cultured for another 4 h

(GST-PIMs) or 24 h (GST-LDHAs). For some of the experiments as indicated, the GST tag was removed using the Pierce™ HRV 3C Protease Solution Kit (Thermo Scientific 88947) according to the manufacturer's protocol. The following purification steps of GST-tagged proteins have been described previously [12].

Western blotting

Cells were lysed for 10 min in ice-cold 50 mM Tris–HCl, pH 8.0, buffer containing 150 mM NaCl, 2 mM EDTA, 1% NP-40, 5 mM NaF, 1 mM Na_3VO_4, 1 mM PMSF, 2 μg·mL^{-1} leupeptin, aprotinin, pepstatin A, 5 mM NEM, 5 mM chloroacetamide and Mini EDTA-free protease inhibitor tablet (Roche, Basel, Switzerland). Cell lysates were sonicated for 1 min and supernatants were collected after 5 min of centrifugation at 21 000 × *g*. Protein concentrations were determined using the Bio-Rad Protein Assay Dye Reagent or Pierce™ BCA Protein Assay Kit according to manufacturers' protocols. Protein aliquots (20–90 μg) were separated by 10% SDS/PAGE and transferred onto a PVDF membrane (Millipore, Burlington, MA, USA). The membranes were incubated overnight at +4 °C with primary antibodies (Table S2). Secondary antibody staining (1 : 5000) was performed for 1 h at RT with HRP-linked goat anti-mouse IgG #7076 or goat anti-rabbit IgG #7074 antibodies (Cell Signalling Technology, Beverly, MA, USA).

For immunoprecipitation experiments with ubiquitin, SDS concentration in the lysis buffer was adjusted to 1% prior to sonication. After sonication, the lysates were diluted to 0.1% SDS before loading onto the agarose beads. For immunoprecipitation of endogenous proteins, antibodies were incubated with protein G agarose (Thermo Scientific #20398) overnight at +4 °C, washed twice with lysis buffer and incubated with protein lysates. For immunoprecipitation of Flag-tagged proteins, 0.2–1 mg aliquots of protein lysates were incubated with 10 μL of anti-Flag® M2 affinity agarose gel (#A2220, Sigma-Aldrich). After 1 h incubation with rotation at +4 °C, the agarose gel was washed three times with the lysis buffer. Samples were prepared for western blotting by adding 2× Laemmli sample buffer directly to the agarose gel and by heating the samples for 10 min at +95 °C prior to gel loading. Chemiluminescence was detected by Bio-Rad Clarity or Clarity Max ECL western blotting substrates. Results were visualized with the ChemiDoc™ MP Imaging System and analysed with IMAGE LAB software Version 5.2.1 (Bio-Rad Laboratories, Inc., Hercules, CA, USA).

cDNA synthesis and quantitative RT-PCR

Cells were lysed directly with TRIzol™ Reagent (Thermo Fisher) and RNA samples were extracted according to the manufacturer's protocol. Prior to cDNA synthesis, samples

were treated with RNase-free DNase 1 (Thermo Scientific EN0521) to ensure the complete absence of DNA. cDNA was synthesized from 1 ug RNA using RevertAid First Strand cDNA Synthesis Kit (Thermo Scientific K1622) according to the manufacturer's protocol. Quantitative RT-PCR was carried out in Mic qPCR Cycler (Bio Molecular Systems) with GoTaq® qPCR Master Mix (Promega) according to the manufacturer's protocol. The primers were synthesized by Integrated DNA Technologies (Table S3). The fold change of gene expression was normalized with ACTB and calculated using the $2^{-\Delta\Delta CT}$ method [54].

Nuclear/Cytoplasmic fractionation

Nearly confluent cells (~ 80% confluence) were collected from 10 cm plates by scraping them into 1 mL aliquots of PBS. After 10 s centrifugation at 21 000 × g, supernatants were discarded and the pellets were lysed for 15 min in 500 μL of lysis buffer: 10 mM Tris–HCl, pH 7.5, 10 mM NaCl, 3 mM MgCl$_2$, 0.5% Nonidet P-40, 5 mM NaF, 1 mM PMSF, 2 μg·mL^{-1} leupeptin, aprotinin and pepstatin A, 5 mM NEM, 5 mM chloroacetamide and mini-EDTA-free protease inhibitor tablet. After centrifugation at 500 × g for 5 min at +4 °C, the supernatants contained the cytoplasmic compartments, while the nuclei were in the pellets. The pellets were washed three times with 500 μL lysis buffer and centrifuged each time at 500 × g for 5 min at +4 °C, after which they were suspended in 200 μL of lysis buffer and sonicated for 30 s. After additional centrifugation at 500 × g for 1 min, the supernatants were collected which contained nuclear fractions. The cytoplasm-containing solutions were centrifuged at 12 000 × g for 15 min at +4 °C, after which the supernatant was collected. Lamin A/C or Lamin A and beta-tubulin were used as nuclear and cytosolic markers, respectively, to evaluate fractionation efficiency.

In vitro kinase assays and mass spectrometry of phosphorylated substrates

The procedure for performing radioactive *in vitro* kinase assays has previously been described [55]. Briefly, 0.5–2.0 μg of PIM kinases and their substrates were used in each reaction. Samples were separated by SDS/PAGE and stained with Page Blue™ protein staining solution (#24620, Thermo Fisher Scientific). Band intensities were quantitated by the IMAGE LAB software Version 5.2.1 (Bio-Rad). For mass spectrometry analyses of phosphorylated substrates, additional *in vitro* kinase assays were performed similarly but with the use of non-radioactive ATP. Protein bands were visualized by ProQ® Diamond Phosphoprotein Gel Stain (Thermo Fisher Scientific) after SDS/PAGE. In-gel digestion of proteins with trypsin, liquid chromatography–electrospray ionization–tandem mass spectrometry (LC-ESI-MS/MS) with phosphopeptide enrichment and data analysis have been previously described [56,57].

Enzymatic assays

Lactate dehydrogenase enzyme activities were measured as previously described [23] but with slight modifications. Cells were lysed in nuclear/cytoplasmic fractionation buffer and separated into whole cell lysate, cytosolic fraction and nuclear fraction. Protein concentrations for each fraction were determined using the Pierce™ BCA Protein Assay Kit according to manufacturers' protocols. Aliquots of protein from whole-cell lysates (2 μg), cytosolic fractions (2 μg) and nuclear fractions (60 μg) were added into the reaction mixture buffer that consisted of 50 mM Tris–HCl, pH 7.4, 20 μM NADH, and 3.3 mM pyruvate (or 3.3 mM sodium 2-ketobutyrate) in a total volume of 200 μL. LDHA activities were measured by the decrease in fluorescence (Ex. 350 nm, Em. 470 nm) corresponding to the conversion of NADH to NAD$^+$ at 25 °C, and normalized to the amount of LDHA protein.

Proximity ligation assay (PLA)

Cell samples seeded on coverslips were fixed for 10 min with 4% paraformaldehyde, washed twice with PBS, once with 0.1% Triton X-100 in PBS for 10 min and twice with PBS. Thereafter, the assays were continued using the Duolink® *In Situ* Detection Reagent kit (DUO9207, Sigma-Aldrich) according to manufacturer's instructions. Samples were imaged by the Nikon fluorescent microscope with NIS-Elements AR software (Nikon, Tokyo, Japan) and analysed by IMAGEJ/FIJI (Wayne Rasband, National Institutes of Health, Bethesda, MD, USA).

Protein crosslinking assay

Cells were lysed in a buffer containing 40 mM HEPES pH 7.5, 150 mM NaCl, 0.1% NP-40, 1 mM PMSF, 2 μg·mL^{-1} leupeptin, aprotinin and pepstatin A and mini-EDTA-free protease inhibitor tablet. After 30 min of centrifugation at 16 000 × g, supernatants were collected and protein concentrations were determined using the Pierce™ BCA Protein Assay Kit. For crosslinking reactions, 100 μg aliquots of protein were incubated with glutaraldehyde (final concentration 0.0625%; Sigma-Aldrich) for 10 min at 25 °C or 30 °C, followed by the addition of glycine (final concentration 50 mM) for 10 min to terminate the reactions. Samples were then subjected to SDS/PAGE analysis.

Statistical analysis and figure preparation

Bar charts were produced using GRAPHPAD PRISM 6.0 (GraphPad Software, San Diego, CA, USA) and the results were analysed using Student's *t*-test. Significant differences ($P < 0.05$ and $P < 0.01$) were marked with * and ** respectively. Error bars represent standard deviations. Inkscape was used for figure preparation.

Acknowledgements

Conflict of interest

The authors declare no conflict of interest.

Author contributions

The study was designed and written by KLM and PJK. Experiments were performed by KLM. AM provided expertise and reagents for ubiquitination assays. All authors have read and approved the manuscript.

Peer review

The peer review history for this article is available at https://publons.com/publon/10.1111/febs.16653.

Data availability statement

The data that support the findings of this study are available from the corresponding author (paivi.koskinen@utu.fi) upon reasonable request.

References

1 Brault L, Gasser C, Bracher F, Huber K, Knapp S, Schwaller J. PIM serine/threonine kinases in the pathogenesis and therapy of hematologic malignancies and solid cancers. *Haematologica*. 2010;**95**:1004–15.

2 Brasó-Maristany F, Filosto S, Catchpole S, Marlow R, Quist J, Francesch-Domenech E, et al. PIM1 kinase regulates cell death, tumor growth and chemotherapy response in triple-negative breast cancer. *Nat Med*. 2016;**22**:1303–13.

3 Eerola SK, Kohvakka A, Tammela TLJ, Koskinen PJ, Latonen L, Visakorpi T. Expression and ERG regulation of PIM kinases in prostate cancer. *Cancer Med*. 2021;**10**:3427–36.

4 Nawijn MC, Alendar A, Berns A. For better or for worse: the role of Pim oncogenes in tumorigenesis. *Nat Rev Cancer*. 2011;**11**:23–34.

5 Warfel NA, Kraft AS. PIM kinase (and Akt) biology and signaling in tumors. *Pharmacol Ther*. 2015;**151**:41–9.

6 Santio NM, Koskinen PJ. PIM kinases: From survival factors to regulators of cell motility. *Int J Biochem Cell Biol*. 2017;**93**:74–85.

7 Qian KC, Wang L, Hickey ER, Studts J, Barringer K, Peng C, et al. Structural basis of constitutive activity and a unique nucleotide binding mode of human Pim-1 kinase. *J Biol Chem*. 2005;**280**:6130–7.

8 Aho TLT, Sandholm J, Peltola KJ, Mankonen HP, Lilly M, Koskinen PJ. Pim-1 kinase promotes inactivation of the pro-apoptotic Bad protein by phosphorylating it on the Ser112 gatekeeper site. *FEBS Lett*. 2004;**571**:43–9.

9 Eerola SK, Santio NM, Rinne S, Kouvonen P, Corthals GL, Scaravilli M, et al. Phosphorylation of NFATC1 at PIM1 target sites is essential for its ability to promote prostate cancer cell migration and invasion. *Cell Commun Signal*. 2019;**17**:148.

10 Santio NM, Landor SK-J, Vahtera L, Ylä-Pelto J, Paloniemi E, Imanishi SY, et al. Phosphorylation of Notch1 by Pim kinases promotes oncogenic signaling in breast and prostate cancer cells. *Oncotarget*. 2016;**7**:43220–38.

11 Landor SKJ, Santio NM, Eccleshall WB, Paramonov VM, Gagliani EK, Hall D, et al. PIM-induced phosphorylation of Notch3 promotes breast cancer tumorigenicity in a CSL-independent fashion. *J Biol Chem*. 2021;**296**:100593.

12 Santio NM, Vainio V, Hoikkala T, Mung KL, Lång M, Vahakoski R, et al. PIM1 accelerates prostate cancer cell motility by phosphorylating actin capping proteins. *Cell Commun Signal*. 2020;**18**:121.

13 Mung KL, Eccleshall WB, Santio NM, Rivero-Müller A, Koskinen PJ. PIM kinases inhibit AMPK activation and promote tumorigenicity by phosphorylating LKB1. *Cell Commun Signal*. 2021;**19**(1):68.

14 Beharry Z, Mahajan S, Zemskova M, Lin Y-W, Tholanikunnel BG, Xia Z, et al. The Pim protein kinases regulate energy metabolism and cell growth. *Proc Natl Acad Sci USA*. 2011;**108**:528–33.

15 Song JH, An N, Chatterjee S, Kistner-Griffin E, Mahajan S, Mehrotra S, et al. Deletion of Pim kinases elevates the cellular levels of reactive oxygen species and sensitizes to K-Ras-induced cell killing. *Oncogene*. 2015;**34**:3728–36.

16 Din S, Konstandin MH, Johnson B, Emathinger J, Völkers M, Toko H, et al. Metabolic dysfunction

consistent with premature aging results from deletion of Pim kinases. *Circ Res.* 2014;**115**:376–87.

17 Hoover D, Friedmann M, Reeves R, Magnuson NS. Recombinant human Pim-1 protein exhibits serine/threonine kinase activity. *J Biol Chem.* 1991;**266**: 14018–23.

18 Yu Z, Zhao X, Huang L, Zhang T, Yang F, Xie L, et al. Proviral insertion in murine lymphomas 2 (PIM2) oncogene phosphorylates pyruvate kinase M2 (PKM2) and promotes glycolysis in cancer cells. *J Biol Chem.* 2013;**288**:35406–16.

19 Yang T, Ren C, Qiao P, Han X, Wang L, Lv S, et al. PIM2-mediated phosphorylation of hexokinase 2 is critical for tumor growth and paclitaxel resistance in breast cancer. *Oncogene.* 2018;**37**:5997–6009.

20 Casillas AL, Chauhan SS, Toth RK, Sainz AG, Clements AN, Jensen CC, et al. Direct phosphorylation and stabilization of HIF-1α by PIM1 kinase drives angiogenesis in solid tumors. *Oncogene.* 2021;**40**: 5142–52.

21 Leverson JD, Koskinen PJ, Orrico FC, Rainio EM, Jalkanen KJ, Dash AB, et al. Pim-1 kinase and p100 cooperate to enhance c-Myb activity. *Mol Cell.* 1998;**2**:417–25.

22 Mishra D, Banerjee D. Lactate dehydrogenases as metabolic links between tumor and stroma in the tumor microenvironment. *Cancer.* 2019;**11**:750.

23 Liu Y, Guo J-Z, Liu Y, Wang K, Ding W, Wang H, et al. Nuclear lactate dehydrogenase A senses ROS to produce α-hydroxybutyrate for HPV-induced cervical tumor growth. *Nat Commun.* 2018;**9**:4429.

24 Stambaugh R, Post D. Substrate and product inhibition of rabbit muscle lactic dehydrogenase heart (H4) and muscle (M4) isozymes. *J Biol Chem.* 1966;**241**: 1462–7.

25 Koukourakis MI, Giatromanolaki A, Sivridis E, Bougioukas G, Didilis V, Gatter KC, et al. Lactate dehydrogenase-5 (LDH-5) overexpression in non-small-cell lung cancer tissues is linked to tumour hypoxia, angiogenic factor production and poor prognosis. *Br J Cancer.* 2003;**89**:877–85.

26 Rong Y, Wu W, Ni X, Kuang T, Jin D, Wang D, et al. Lactate dehydrogenase A is overexpressed in pancreatic cancer and promotes the growth of pancreatic cancer cells. *Tumour Biol.* 2013;**34**:1523–30.

27 Koukourakis MI, Giatromanolaki A, Panteliadou M, Pouliliou SE, Chondrou PS, Mavropoulou S, et al. Lactate dehydrogenase 5 isoenzyme overexpression defines resistance of prostate cancer to radiotherapy. *Br J Cancer.* 2014;**110**:2217–23.

28 Koukourakis MI, Giatromanolaki A, Sivridis E. Lactate dehydrogenase Isoenzymes 1 and 5: differential expression by neoplastic and stromal cells in non-small cell lung cancer and other epithelial malignant tumors. *Tumor Biol.* 2003;**24**:199–202.

29 Dennison JB, Molina JR, Mitra S, González-Angulo AM, Balko JM, Kuba MG, et al. Lactate dehydrogenase B: a metabolic marker of response to neoadjuvant chemotherapy in breast cancer. *Clin Cancer Res.* 2013;**19**:3703–13.

30 McCleland ML, Adler AS, Shang Y, Hunsaker T, Truong T, Peterson D, et al. An integrated genomic screen identifies LDHB as an essential gene for triple-negative breast cancer. *Cancer Res.* 2012;**72**:5812–23.

31 Zhao D, Zou S-W, Liu Y, Zhou X, Mo Y, Wang P, et al. Lysine-5 acetylation negatively regulates lactate dehydrogenase A and is decreased in pancreatic cancer. *Cancer Cell.* 2013;**23**:464–76.

32 Li X, Zhang C, Zhao T, Su Z, Li M, Hu J, et al. Lysine-222 succinylation reduces lysosomal degradation of lactate dehydrogenase a and is increased in gastric cancer. *J Exp Clin Cancer Res.* 2020;**39**:172.

33 Fan J, Hitosugi T, Chung T-W, Xie J, Ge Q, Gu T-L, et al. Tyrosine phosphorylation of lactate dehydrogenase A is important for NADH/NAD+ redox homeostasis in cancer cells. *Mol Cell Biol.* 2011;**31**:4938–50.

34 Jin L, Chun J, Pan C, Alesi G, Li D, Magliocca K, et al. Phosphorylation-mediated activation of LDHA promotes cancer cell invasion and tumour metastasis. *Oncogene.* 2017;**36**:3797–806.

35 Zhong X, Tian S, Zhang X, Diao X, Dong F, Yang J, et al. CUE domain-containing protein 2 promotes the Warburg effect and tumorigenesis. *EMBO Rep.* 2017;**18**:809–25.

36 Muslin AJ, Tanner JW, Allen PM, Shaw AS. Interaction of 14-3-3 with signaling proteins is mediated by the recognition of phosphoserine. *Cell.* 1996;**84**: 889–97.

37 Fu H, Subramanian RR, Masters SC. 14-3-3 proteins: structure, function, and regulation. *Annu Rev Pharmacol Toxicol.* 2000;**40**:617–47.

38 Pennington KL, Chan TY, Torres MP, Andersen JL. The dynamic and stress-adaptive signaling hub of 14-3-3: emerging mechanisms of regulation and context-dependent protein–protein interactions. *Oncogene.* 2018;**37**:5587–604.

39 Macdonald A, Campbell DG, Toth R, McLauchlan H, Hastie CJ, Arthur JSC. Pim kinases phosphorylate multiple sites on Bad and promote 14-3-3 binding and dissociation from Bcl-XL. *BMC Cell Biol.* 2006;**7**:1.

40 Peng C, Knebel A, Morrice NA, Li X, Barringer K, Li J, et al. Pim kinase substrate identification and specificity. *J Biochem (Tokyo).* 2007;**141**:353–62.

41 Komander D, Rape M. The ubiquitin code. *Annu Rev Biochem.* 2012;**81**:203–29.

42 Cooper JA, Reiss NA, Schwartz RJ, Schwartz RJ, Schwartz RJ, Hunter T. Three glycolytic enzymes are phosphorylated at tyrosine in cells transformed by Rous sarcoma virus. *Nature.* 1983;**302**:1–223.

43 Zhong XH, Howard BD. Phosphotyrosine-containing lactate dehydrogenase is restricted to the nuclei of PC12 pheochromocytoma cells. *Mol Cell Biol*. 1990;**10**:770–6.

44 Chen Y-J, Mahieu NG, Huang X, Singh M, Crawford PA, Johnson SL, et al. Lactate metabolism is associated with mammalian mitochondria. *Nat Chem Biol*. 2016;**12**:937–43.

45 Hornbeck PV, Zhang B, Murray B, Kornhauser JM, Latham V, Skrzypek E. PhosphoSitePlus, 2014: mutations, PTMs and recalibrations. *Nucleic Acids Res*. 2015;**43**:D512–20.

46 Onishi Y, Hirasaka K, Ishihara I, Oarada M, Goto J, Ogawa T, et al. Identification of mono-ubiquitinated LDH-A in skeletal muscle cells exposed to oxidative stress. *Biochem Biophys Res Commun*. 2005;**336**:799–806.

47 Maitland MER, Kuljanin M, Wang X, Lajoie GA, Schild-Poulter C. Proteomic analysis of ubiquitination substrates reveals a CTLH E3 ligase complex-dependent regulation of glycolysis. *FASEB J*. 2021;**35**:e21825.

48 Dar A, Wu D, Lee N, Shibata E, Dutta A. 14-3-3 proteins play a role in the cell cycle by shielding Cdt2 from ubiquitin-mediated degradation. *Mol Cell Biol*. 2014;**34**:4049–61.

49 Dai R-P, Yu F-X, Goh S-R, Chng H-W, Tan Y-L, Fu J-L, et al. Histone 2B (H2B) expression is confined to a proper NAD+/NADH redox status*. *J Biol Chem*. 2008;**283**:26894–901.

50 He H, Lee M-C, Zheng L-L, Zheng L, Luo Y. Integration of the metabolic/redox state, histone gene switching, DNA replication and S-phase progression by moonlighting metabolic enzymes. *Biosci Rep*. 2013;**33**:e00018.

51 Zhang D, Tang Z, Huang H, Zhou G, Cui C, Weng Y, et al. Metabolic regulation of gene expression by histone lactylation. *Nature*. 2019;**574**:575–80.

52 Yu J, Chai P, Xie M, Ge S, Ruan J, Fan X, et al. Histone lactylation drives oncogenesis by facilitating m6A reader protein YTHDF2 expression in ocular melanoma. *Genome Biol*. 2021;**22**:85.

53 Santio NM, Eerola SK, Paatero I, Yli-Kauhaluoma J, Anizon F, Moreau P, et al. Pim kinases promote migration and metastatic growth of prostate cancer xenografts. *PLoS ONE*. 2015;**10**:e0130340.

54 Livak KJ, Schmittgen TD. Analysis of relative gene expression data using real-time quantitative PCR and the $2-\Delta\Delta CT$ method. *Methods*. 2001;**25**:402–8.

55 Kiriazis A, Vahakoski RL, Santio NM, Arnaudova R, Eerola SK, Rainio EM, et al. Tricyclic benzo[cd] azulenes selectively inhibit activities of Pim kinases and restrict growth of Epstein-Barr virus-transformed cells. *PLoS ONE*. 2013;**8**:e55409.

56 Kauko O, Laajala TD, Jumppanen M, Hintsanen P, Suni V, Haapaniemi P, et al. Label-free quantitative phosphoproteomics with novel pairwise abundance normalization reveals synergistic RAS and CIP2A signaling. *Sci Rep*. 2015;**5**:13099.

57 Imanishi SY, Kochin V, Eriksson JE. Optimization of phosphopeptide elution conditions in immobilized Fe (III) affinity chromatography. *Proteomics*. 2007;**7**:174–6.

Supporting information

Additional supporting information may be found online in the Supporting Information section at the end of the article.

Table S1. List of primers for LDHA plasmid mutagenesis.
Table S2. List of antibodies used in the experiments.
Table S3. List of primers for PCR.